Triplet generation and upper critical field in superconducting spin valves based on CrO_2

S. Voltan, A. Singh, and J. Aarts
Huygens-Kamerlingh Onnes Laboratory, Leiden University, Post Office Box 9504, 2300 RA Leiden, The Netherlands
(Received 16 April 2016; revised manuscript received 22 June 2016; published 4 August 2016)

It has been recently reported that a superconducting triplet spin valve (TSV) based on the half-metallic CrO_2 can show "colossal" variations of the critical temperature, up to more than 1 K. This can be achieved when the magnetic noncollinearity between the mixer (F_1) and the drainage ferromagnetic layer (F) is maximized. In this work we investigate further such TSV devices looking at two aspects: first, we present the dependence of the TSV effect on the thickness of the mixer layer; second, we look at the perpendicular upper critical field $H_{c2\perp}$ as a function of the temperature. The thickness dependence, which is nonmonotonic as expected, represents a further proof that the effect is due to the generation of equal-spin triplet Cooper pairs, while what we observe for the $H_{c2\perp}$ versus T curves is an interesting and peculiar behavior: there is a clear deviation from the universal linear dependence and the average slope is suppressed much more than what can be described with the formalism used for conventional proximized structures.

DOI: 10.1103/PhysRevB.94.054503

I. INTRODUCTION

Ferromagnetism and superconductivity are mutually exclusive states because of the inherent competition between the exchange energy, which aligns the spins parallel, and the superconducting pairing, which aligns them antiparallel. However, supercurrents can be injected from a superconductor (S) into a ferromagnet (F) and survive for surprisingly long distances. This is possible only if conventional singlet Cooper pairs are converted into more unconventional triplet ones, with the spins aligned parallel and therefore not affected by the exchange interaction. In this case the limiting factors for the propagation in the F layer are temperature and spin-diffusion length. In a standard ferromagnet, such as Co, the spin-diffusion length is about 60 nm, while in a half-metallic ferromagnet, with full spin polarization such as CrO_2, triplet Cooper pairs can survive for distances up to several hundred nm [1,2]. In a half-metal (HM), indeed, at the Fermi level only one spin band is available and so at low temperatures no spin-flip scattering event, which would break the Cooper pairs, is allowed. These distances are remarkably larger than the characteristic short-range penetration lengths of the singlet component: about 1–2 nm for standard ferromagnets, atomic lengths for half-metals. In the case of half-metals not only are the injected superconducting correlations long range but they are also fully spin polarized, which makes CrO_2-based devices appealing systems to develop superconducting spintronics applications [3].

The mechanism which converts the singlet into an equal-spin triplet is realized at the S/F interface in two steps: a spin mixing process followed by spin rotation [4–6]. The spin rotation converts the $m_s = 0$ triplet component ($\uparrow\downarrow + \downarrow\uparrow$), generated by the spin mixing, into the parallel-spin triplet $m_s = 1$ component ($\uparrow\uparrow$). This conversion is possible if some sort of magnetic inhomogeneity is provided at the S/F interface. In the past decade many experimental works [1,2,7–9] unequivocally showed evidence of a long-range proximity effect in S/F/S Josephson junctions. In most of these experiments the magnetic inhomogeneity was engineered by introducing an extra thin ferromagnetic layer F_1 between S and F on both sides. If the magnetization directions of F and F_1 are misaligned there is triplet generation. The crucial role played by the magnetic inhomogeneity was shown in a clear way, validating the theoretical model described above. Furthermore, a theoretical formalism was recently developed to specifically describe the proximity effect in the case of half-metals [10]. However, there are still several open questions about the mechanism and full control of the triplet generation has not been achieved yet.

In the last few years there has been a growing interest in superconducting triplet spin valve (TSV) devices [11], as a useful tool to provide better insight into the triplet generation. A TSV is a multilayer structure S/F_1/N/F, which can be thought of as half of a Josephson Junction with only one interface for singlet to triplet conversion, and therefore easier to control. The thin normal metal layer N is simply used to decouple the magnetizations F_1 and F. When the magnetization of F_1 (called the mixer layer) and F (the drainage layer) are noncollinear, there is generation of long-range triplets. The leakage of Cooper pairs into F results in a decrease of the superconducting order parameter of the S layer, and a drop of T_c, provided that the S layer is not thicker than a few times the superconducting coherence length ξ_S. The maximum efficiency of triplet generation, so the biggest suppression, is reached when the angle between the two magnetization directions is 90 deg.

HMs form a special class of ferromagnets, with clear relevance for triplet proximity effects. In our recent work [12], by using TSVs based on the half-metallic CrO_2 we could show a huge T_c suppression, well over 1 K. Such a large effect is more than an order of magnitude bigger than for TSVs based on standard ferromagnets [13–15]. An explanation for this was recently given by Mironov and Buzdin [16], who showed that the special boundary conditions for a S/F/HM system (as opposed to an S/F_1/F_2 system) lead to the appearance of an extra triplet component in the S and F layers, with a much stronger effect on T_c of the spin valve as a consequence.

In the experiments presented in Ref. [12] we have to keep in mind that, to induce the magnetic noncollinearity between F_1 and F, the magnetic field was rotated from in-plane to out-of-plane. For this reason we had to ascertain that the measured δT_c was not due to the difference between the parallel and perpendicular upper critical field H_{c2}. In particular, in the

out-of-plane configuration, several spurious effects such as vortices and stray field of the magnetic layers can influence the superconducting properties. In Ref. [12] this problem was circumvented by comparing the behavior of the TSV to equivalent structures where either the F_1 or the F layer was removed, so where the triplet generation was not expected. However, measuring H_{c2} as a function of temperature would actually provide a more fundamental description of the TSV effect. The study of H_{c2} not only quantifies the efficiency of triplet generation but also probes the change in behavior of the superconductor due to the triplet proximity effect.

In this paper we study CrO_2-based TSVs similar to the ones studied in Ref. [12], with MoGe as S layer and Ni as mixer layer, looking at two aspects not explored so far. First we study the dependence of the TSV efficiency on the Ni thickness. From the theoretical framework we know that there should be an optimum thickness for the mixer layer. Indeed, since the equal-spin triplet component is generated starting from the $m_s = 0$ component created in the mixer layer, it follows that this layer has to be thick enough to give a sufficient amplitude of the $m_s = 0$ component, but thinner than the decay length (a few nm). Here we confirm that there is a nonmonotonic dependence with the optimum thickness value around 1.5 nm. The result is consistent with previous studies of a Ni mixer layer in Josephson junctions based on Co [8], and also consistent with the theoretical results of Ref. [16]. It is a further proof, even if indirect, that the observed TSV effect is due to triplet generation.

The second point we address is the effect of the triplet generation on the phase diagram of the superconductor $H_{c2\perp}(T)$. For the reasons explained above, $H_{c2\perp}(T)$ of the stack seems to be a more fundamental quantity to study the TSVs, particularly in our device geometry. With the field applied out-of-plane (the TSV is "on") we observe an unexpected behavior: the $H_{c2\perp}(T)$ phase diagram strongly deviates from the universal linear behavior observed for both isolated superconductors and structures with no triplet generation. Next to that, there is a strong suppression of the critical field, namely, a decrease of the average slope, which cannot be described with the standard formalism for proximized S/F hybrids. The link between triplet generation and $H_{c2\perp}(T)$ dependence is confirmed by comparing TSVs with different Ni thickness, so with different efficiency in triplet generation. We show how this reflects in a very different critical field behavior, the study of which can be used to have insightful information about the triplet generation.

In Sec. II we describe sample preparation and measurement details while in Sec. III we present the results on the T_c variation as a function of the spin mixer thickness (A) and we discuss the features due to spin accumulation; in Sec. IV we show the results for the temperature dependence of the perpendicular upper critical field for the TSVs (B) compared with the isolated superconductor and the S/F hybrids in absence of triplet generation (A). To conclude, in Sec. V we highlight the main results of our study.

II. SAMPLE PREPARATION AND EXPERIMENTS

Our TSV device is a stack of four layers, namely, $Mo_{70}Ge_{30}(25)/Ni(d_{Ni})/Cu(5)/CrO_2(100)$ [Fig. 1(b)], where the numbers express the thickness in nanometers. For simplicity

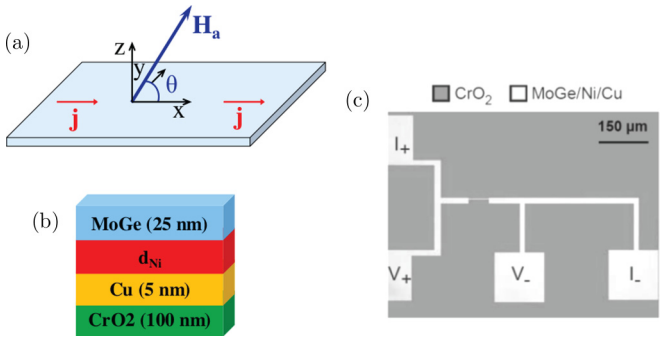

FIG. 1. (a) Coordinate system used in angle dependent magnetotransport measurements, showing the direction of the current j, the applied field H_a, and the angle θ between them. (b) Sketch which shows the four layers forming the TSV, with their respective thickness. (c) Optical micrograph of a typical TSV where a MoGe/Ni/Cu trilayer bridge of 10-μm width was patterned on a film of CrO_2. The thicknesses of the different layers are the same as in (b). d_{Ni} was varied, with values $d_{Ni} = 0$, 1.0, 1.5, 2.2, and 3.0 nm.

$Mo_{70}Ge_{30}$ is called MoGe. Via sputtering and liftoff the trilayer MoGe/Ni/Cu was patterned in a four-terminal structure with a bridge 10 μm wide on top of a CrO_2 film grown by chemical vapor deposition on a crystalline TiO_2 (100) substrate. More details about the film growth can be found in Ref. [12] (Supplemental Material). An optical image of a typical device is shown in Fig. 1(c). The bridge direction is parallel to the magnetic easy axis of CrO_2, which is along the c-(001) direction of the TiO_2 surface. Right before the deposition of the trilayer, CrO_2 was Ar etched in order to remove the native Cr_2O_3 oxide from the surface. The importance of this step, fundamental to achieve a good interface transparency, has been extensively discussed in Ref. [12]. The thickness of the mixer layer was varied, with values $d_{Ni} = 0$, 1.0, 1.5, 2.2, and 3.0 nm. We performed electrical measurements in a physical properties measurement system. The angle θ between the surface plane and the applied magnetic field H_a could be varied. When H_a is rotated out of the plane, the magnetization vectors of both the Ni and the CrO_2 layer are gradually pulled out-of-plane. However, the magnetization loops (presented in Ref. [12]) show a different saturation field for the two ferromagnetic layers, so that at a given field below the saturation there is an angle between the two vectors, meaning the Ni layer has a stronger perpendicular component. This difference accounts for the magnetic noncollinearity. The $R(T)$ curves (Sec. III) were obtained with the magnetic field both in-plane ($\theta = 0°$) and out-of-plane ($\theta = 90°$). The measurement configuration and the definition of θ are represented in the sketch of Fig. 1(a). When H_a is in-plane it is always parallel to the current direction. The $R(H)$ measurements (Sec. IV) were only performed in the out-of-plane configuration. Further details about the measurement setup can be found in Ref. [12].

III. T_c VARIATION IN TRIPLET SPIN VALVES

A. Spin mixer thickness dependence

In this section we present measurements performed on TSVs with different Ni thickness d_{Ni}, in order to study the dependence and to determine the optimum value. We measured

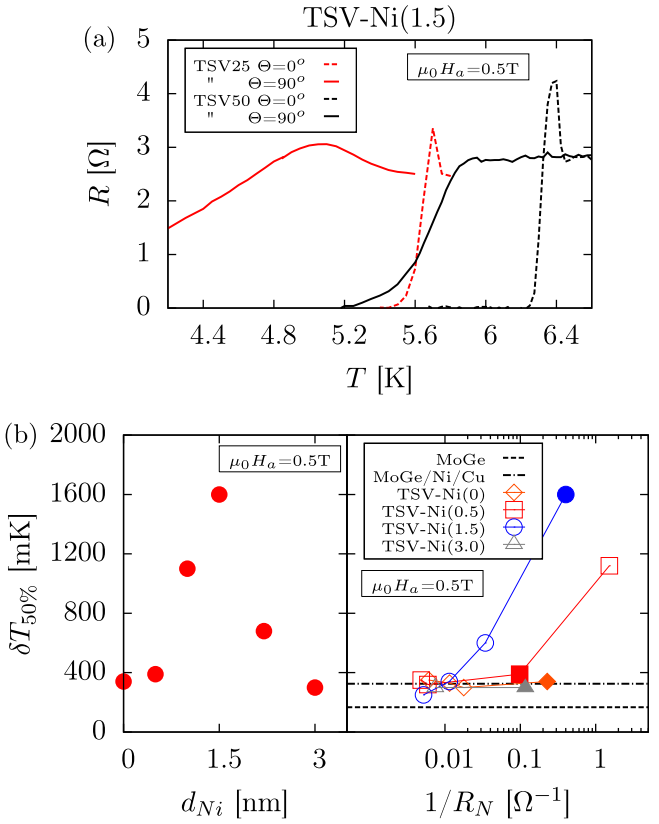

FIG. 2. (a) Transition curves $R(T)$ for two TSVs MoGe(d_S)/Ni(1.5)/Cu(5)/CrO_2(100) with d_S = 25 nm (TSV25, red curves) and 50 nm (TSV50, black curves), in a field of 0.5 T, either applied in-plane (dashed lines) or out-of-plane (full lines). (b) Left panel: Dependence of the TSV efficiency, measured by $\delta T_{50\%,\max} = T_{50\%}(0^\circ) - T_{50\%}(90^\circ)$, for TSV25 devices in a field of 0.5 T, as a function of the thickness of the mixer layer $d_{\rm Ni}$ and (right panel) dependence of the TSV efficiency as a function of the interface transparency, measured by the reciprocal of the normal resistance $1/R_N$, for different series of TSV25s, each with a different $d_{\rm Ni}$ value. Dashed and dash-dotted lines show the $\delta T_{50\%,\max}$ value for the isolated superconductor MoGe(25) and the trilayer MoGe(25)/Ni(1.5)/Cu(5), respectively. The full symbols represent the points used for the plot in the left panel.

the resistive transition of the TSVs as a function of the temperature, with the magnetic field (0.5 T) applied in-plane ($\theta = 0^\circ$) and out-of-plane ($\theta = 90^\circ$). T_c was defined by using the operational parameter $T_{50\%}$, namely, the temperature at 50% of the resistive transition. The maximum $T_{50\%}$ variation, a measurement of the TSV efficiency, is given by $\delta T_{50\%,\max} = T_{50\%}(0^\circ) - T_{50\%}(90^\circ)$, that for simplicity we will call δT_c (for details see Ref. [12] and its Supplemental Material).

In Fig. 2(a) we show the transition curves for two TSVs, with either a 25-nm- (TSV25, red curves) or a 50-nm-thick (TSV50, black curves) superconducting layer. For both TSVs $d_{\rm Ni}$ is 1.5 nm and the R_N values are similar (2.5 and 2.9 Ω, respectively). Dashed and full lines are for $\theta = 0$ and 90°, respectively.

At the onset of the transition there is a small but distinct peak, with resistance exceeding the normal value R_N. By rotating the field from in-plane to out-of-plane, for TSV25 the peak gets slightly reduced and broadened (together with the transition width). For TSV50, instead, the peak is completely suppressed. This feature is likely due to spin accumulation, as proposed in Ref. [12], and will be more extensively discussed in Sec. III B.

As expected, TSV25 shows a lower T_c and, in line with the theory of proximity effect in a TSV, a larger T_c variation. δT_c is about 1.6 K for TSV25 and 0.65 K for TSV50. $T_{50\%}(90^\circ)$ for TSV25 has been extrapolated because at 4.2 K, the minimum temperature we could reach in that particular measurement, the resistance was still slightly above the threshold of 50% of R_N, even if very close. We have to stress that these values result from the triplet leakage added to spurious effects such as vortex resistance and stray fields of the F_1 and F layers. However, as explained in Ref. [12], these effects at 0.5 T do not exceed a few hundred mK. In the left panel of Fig. 2(b) we plot δT_c as a function of $d_{\rm Ni}$ for TSV25s: as expected the TSV efficiency shows a strongly nonmonotonic behavior with a peak centered around 1.5 nm, which confirms that to be the optimum thickness. For both $d_{\rm Ni}$=0 and 3 nm, for which no triplet generation is expected, the measured variation $\delta T_c \simeq$ 350 mK provides us the magnitude of the triplet-independent effects. The interface transparency between the CrO_2 film and the trilayer above has been proven to be a crucial parameter for the injection of the Cooper pairs into the CrO_2 and therefore for the TSV efficiency [12]. The interface transparency is proportional to the reciprocal of the normal resistance $1/R_N$: if the transparency is low, the barrier resistance, in series with the low resistance of CrO_2, is high, and so R_N is also high. For the TSVs of the left panel of Fig. 2(b), the values of R_N are comparable but not fully equal. For this reason, in order to isolate the effect of the variation of the Ni thickness dependence we should compare structures with similar interface transparency, an experimental parameter not controllable with high precision. Nonetheless the differences among the TSVs do not change the qualitative behavior presented. This becomes clear in the right panel of Fig. 2(b), where the δT_c of different series of TSVs is plotted as a function of the interface transparency. Each curve is a series with a different Ni thickness, while the dashed and the dash-dotted horizontal lines show the T_c variation for a single MoGe(25) layer and a MoGe(25)/Ni(1.5)/Cu(5) trilayer, respectively. The full symbols represent the points used for the plot in the left panel [series Ni(1.0) and Ni (2.2) are not presented for clarity but are consistent with the general behavior]. For low transparencies (low $1/R_N$ values) the leakage is suppressed and all the curves approximately converge to the value of the trilayer. Increasing the transparency results in a growing TSV efficiency and the closer the Ni thickness is to the optimum value the stronger the effect. From the plot it is clear that the TSVs with $d_{\rm Ni}$ = 1.5 nm are the most efficient, which is in line with the theoretical result that the optimum lies around $d_{\rm Ni}$=d_F=ξ_F [16].

B. Spin accumulation

In Sec. III A we pointed out that most of the $R(T)$ curves show a peak at the onset of the superconducting transition. This peak is also present at zero field. In the earlier work [12], zero-field peaks were usually not present but that work

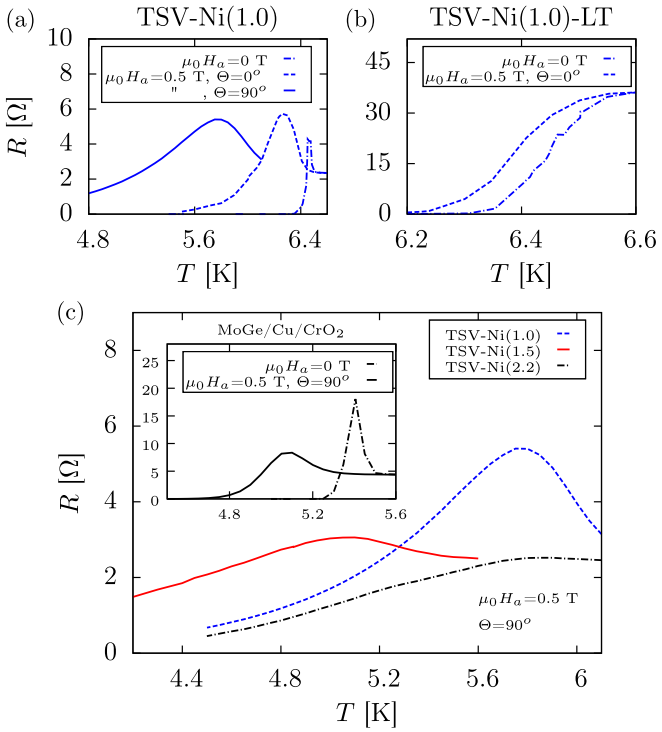

FIG. 3. (a) Transition curves $R(T)$ for a TSV MoGe(25)/Ni(1.5)/Cu(5)/CrO_2(100), at zero field (dot-dashed line) and with a field of 0.5 T applied in plane (dashed line) or out of plane (full line). (b) $R(T)$ curves for a TSV with the same characteristics as in (a), but with a much lower interface transparency. The dot-dashed line is for the measurement at zero field; the dashed line is for the measurement in-field ($\mu_0 H_a = 0.5$ T, in-plane). (c) Spin accumulation peaks at the onset of the R vs T transition in an out-of-plane field of 0.5 T for TSVs with different Ni layer thickness: 1.0 nm (dashed line), 1.5 nm (full line), and 2.2 nm (dot-dashed line). The inset shows the transitions at zero field (dot-dashed line) and in-field out-of-plane (full line) for the trilayer MoGe(25)/Cu(5)/CrO_2(100), with no nickel.

concerned devices with $d_S = 50$ and 25 nm but lower interface transparency. The peak is typically broadened when a field is applied. Furthermore, when we go from an in-plane to an out-of-plane configuration, it gets broader and slightly suppressed. This evolution can be appreciated for the TSV with $d_{Ni} = 1.0$ nm in Fig. 3(a), where we show the transition curves at zero field and 0.5 T, both in-plane and out-of-plane. The normal state resistance for this structure is about 2.4 Ω.

We associate the peak with spin accumulation at the SF'N/F interface. Indeed, right above T_c the current path is mainly confined in the CrO_2 layer, due to its low resistivity. The SF'N/F interface, thus, plays a role in the total measured resistance. At the onset of the superconducting state, triplet Cooper pairs start to be created and, depending on the magnetic configuration of the different layers, at the interface with CrO_2 they can either be injected or broken and reflected as polarized Cooper pairs or polarized quasiparticles. The reflection results in spin accumulation and thus an excess resistance. The dependence of the peak height on the angle of the applied magnetic field makes us discard the charge imbalance as a possible explanation of the observed effect.

For devices in which the interface transparency is lower, the peak is not observed. As an example, in Fig. 3(b) we show the transitions, at zero field (dot-dashed line) and with a field (0.5 T) applied in-plane (dashed line), for a TSV with the same characteristics as in Fig. 3(a) ($d_{Ni} = 1.0$ nm), but with a significantly lower interface transparency, as signaled by the higher R_N value (about 36 Ω). This is, on the one hand, because of the barrier hindering the proximity with CrO_2 and therefore the polarization and, on the other hand, because the higher R_N value makes a contribution coming from the spin accumulation less relevant.

If we compare the transitions for different d_{Ni} values [Fig. 3(c), dashed, full, and dash-dotted line for $d_{Ni} = 1.0$, 1.5, and 2.2 nm, respectively], we see that the relative peak height is increasing with decreasing the Ni thickness, with a maximum height/R_N ratio obtained for the trilayer without nickel (inset). The same trend is observed for the peak at zero field. This is consistent with the spin accumulation mechanism described above: by increasing d_{Ni} we increase the amount of pair breaking inside the nickel layer so that less and less Cooper pairs reach the interface with CrO_2, decreasing the amount of accumulation.

All the TSVs show a slight reduction of the peak height by rotating the field out-of-plane. This can be explained by the fact that when the field is rotated out-of-plane the conditions for the leakage into the CrO_2 layer are optimized and the amount of reflected polarized Cooper pairs (or quasiparticles) is then reduced. In general, to have an exact description of the mechanism responsible for the spin accumulation is not trivial. Indeed, beside F_1 and F, the magnetization of the surface of CrO_2 plays an important role. If residues of the native oxide layer Cr_2O_3 are still present after the Ar-cleaning procedure, there are extra magnetic moments, F′, which can influence the process. The relative orientation of the magnetizations F_1, F′ (if present), and F determines how many singlet Cooper pairs are converted into triplets and how many triplets leak into CrO_2 or are reflected, giving rise to spin accumulation. In a trilayer with no nickel layer, triplets can be generated by the noncollinearity between F′ and F, or simply by the misaligned magnetic moments of the domains of CrO_2, as proposed by previous works [1,2]. In particular, similar peaks were observed for devices MoGe/CrO_2, where the CrO_2 film was grown on sapphire [17] and for Co nanowires contacted by superconducting W bars [18]. This explains why a peak can be observed also for a trilayer MoGe/Cu/CrO_2, both at zero field and in-field [see inset of Fig. 3(c)]. The properties of F′, as well as the interface transparency, are parameters not perfectly controllable. This is a cause of different types of behavior observed for different samples, with respect to peak height or peak evolution from zero field to in-field measurements. In order to achieve a more clear picture about the spin accumulation mechanism further experiments are needed.

IV. PERPENDICULAR UPPER CRITICAL FIELDS $H_{c2\perp}$

Since the changes in T_c as a function of applied field are large, it becomes more reasonable to describe the effects in terms of the critical field H_{c2} of the proximized system, and construct a H_{c2} phase diagram. In our TSVs, beside the

standard (singlet) proximity between the S layer and the F_1/N/F sandwich, there is a triplet channel for the leakage of Cooper pairs which depends on the amount of (in)homogeneity and may therefore depend on H in a nontrivial manner. In that sense the H_{c2} phase diagram will be anomalous because of an underlying change in T_c which is not present in standard proximity systems.

A. $H_{c2\perp}$ of the S layer and of S/F hybrids

We first characterize our system in absence of triplet generation. We measured the resistance versus magnetic field dependence $R(H)$ at different temperatures for (i) a MoGe(25) single film to characterize the isolated superconductor, (ii) a trilayer MoGe(25)/Ni(1.5)/Cu(5), and (iii) a trilayer MoGe(25)/Cu(5)/CrO_2(100) [Figs. 4(a)–4(c), respectively; the numbers in parentheses are the thicknesses in nm]. Cases (ii) and (iii) are studied to look at the pair-breaking effect due to either the Ni or the CrO_2 layer, independently. The Cu layer, used in the TSV only to decouple the ferromagnets, is much thinner than the coherence length ξ_N (of the order of 1 μm) so it does not play a role in suppressing the order parameter. For all the measurements presented in this section the field was applied perpendicular to the plane of the structure, in order to have a reference for the TSV effect, which is maximized when the field is applied in this geometry.

In Fig. 4 we can immediately notice a large difference in the normal resistance R_N of the three structures: 840 Ω for the isolated MoGe [Fig. 4(a)], 240 Ω for the trilayer MoGe/Ni/Cu [Fig. 4(b)], and 4.5 Ω for the trilayer MoGe/Cu/CrO_2 [Fig. 4(c)]. Above T_c, the MoGe has high resistivity ($\rho_{\mathrm{MoGe}} = 200\,\mu\Omega\,\mathrm{cm}$) and therefore is shorted by the Cu layer ($\rho_{\mathrm{Cu}} = 2\,\mu\Omega\,\mathrm{cm}$) in (ii) and by the CrO_2 ($\rho_{\mathrm{CrO_2}} = 6\,\mu\Omega\,\mathrm{cm}$ [19]) in (iii). The low value of R_N for MoGe/Cu/CrO_2 is due to the fact that the CrO_2 is not patterned. In addition it is an indication of a good interface transparency [12]. The peak at the onset of the superconductivity, observed for $R(T)$ curves and discussed in Sec. III B, is clearly visible also for the $R(H)$ curves of the trilayer MoGe/Cu/CrO_2. The peak becomes broader when lowering the temperature.

For the isolated MoGe and the trilayer MoGe/Ni/Cu the value of $H_{c2\perp}$ is extrapolated as shown by the black dashed lines in Fig. 4(a), as the field value at which the fitting line of the linear part of the transition intersects the R_N value. This is a standard construction for cases when the S layer is weakly pinning and freely flowing vortices lead to a flux flow resistance $\rho_f = H/H_{c2}\,\rho_N$ [20].

For the trilayer MoGe/Cu/CrO_2 [see Fig. 4(c)], the shape of the transition is very different because of the feature described in Sec. III B. In addition it is important to point out that the total resistance we measure is the result of the parallel between MoGe which is highly resistive and the other layers. The contribution to the resistance due to vortex motion is $R_f = R_N B/B_{c2}$. In the normal state, the resistance of the superconducting layer R_N is about 840 Ω and it is shorted by the low resistive CrO_2 layer ($R_{\mathrm{CrO_2}} \simeq 2$ Ω). Therefore for the stack MoGe/Cu/CrO_2 (and the TSVs) only the lowest fraction (0.2%) of vortex resistance contributes to the total resistance in the observed transitions. In this region the flow of vortices is not coherent and the dependence of the resistance

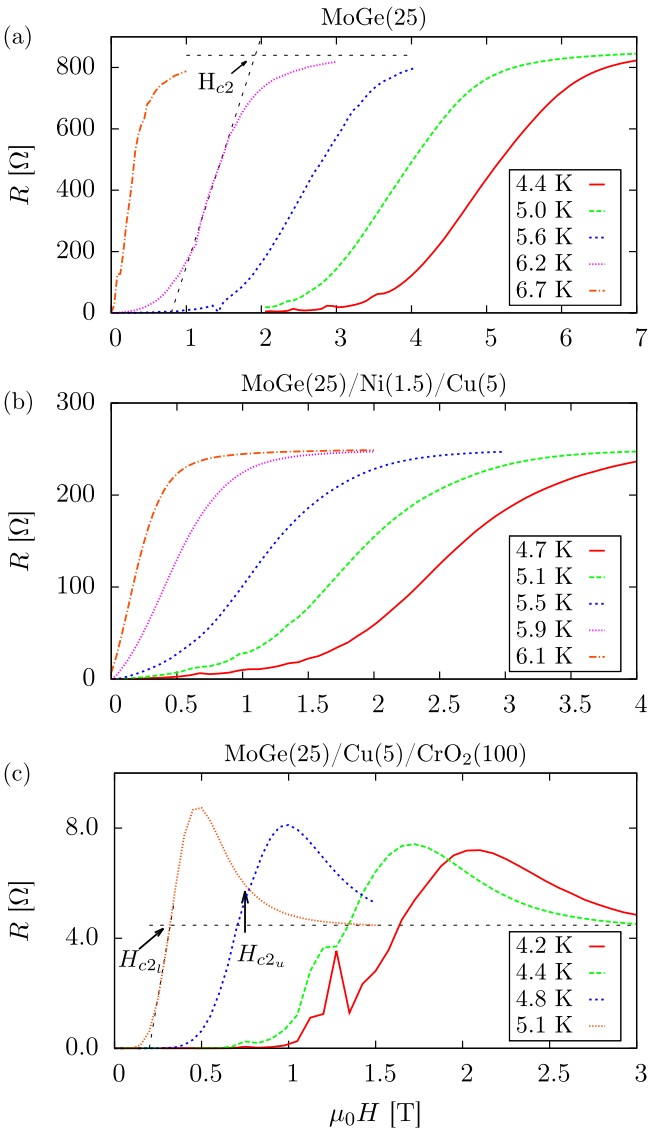

FIG. 4. Plots of the resistance as a function of the magnetic field (applied out-of-plane) at different temperatures for (a) an isolated superconductor MoGe(25), (b) a trilayer MoGe(25)/Ni(1.5)/Cu(5), and (c) a trilayer MoGe(25)/Cu(5)/CrO_2(100). Dashed black lines in (a) and (c) show how the upper critical field $H_{c2\perp}$ has been defined: as the field value at which the fitting line of the linear part of the transition intersects the R_N value.

on the magnetic field is not linear. For this reason the method shown in Fig. 4(a) is no longer justified to determine H_{c2}, also because too little is known about vortex dynamics in proximized systems. The only reliable way we have in this case to define $H_{c2\perp}$ is to consider the field at which, coming from the normal state, the resistance starts to increase as shown in Fig. 4(c) (H_{c2_u} value). The operational threshold is 0.3 times the peak height above the normal value R_N, namely, $R_N + 0.3(R_{\mathrm{max}} - R_N)$, where R_{max} is the maximum resistance value of the peak. As explained above, the peak originates from the breaking of Cooper pairs and starts to set in at the onset of superconductivity, even if not necessarily of the proximity effect. Therefore this value, which we call H_{c2_u}, is an upper limit for the real upper critical field, which could be a bit

lower. For comparison we also look at the dependence of the field value defined as in Fig. 4(a), because only below this value the resistance drops to zero. This value, which we call H_{c2_l} [see Fig. 4(c)], represents a lower limit for the real $H_{c2\perp}$. Also, representing the onset of flux flow, it is definitely related to $H_{c2\perp}$.

Very small oscillations, possibly due to vortex dynamics, are visible at high fields in the tail of the transition curve for the lowest temperatures in Figs. 4(a) and 4(b). The oscillations become much more evident for the trilayer MoGe/Cu/CrO_2 [Fig. 4(c)], in particular at 4.2 and 4.4 K at around 1.2 T. Here the total resistance of the multilayer is low, so the relative contribution of the oscillations, which seems to be of the order of a few ohms, is more relevant. The sharpness of the oscillation at 4.2 K is an artifact due to the limited amount of points acquired for that specific measurement. For the curves where big oscillations are present we fitted the background transition, after subtracting the oscillating contributions. Since the oscillations are superimposed to the resistance curve of the superconductor, they do not contribute to the proximity effect and do not change the slope of the curve, or the value of $H_{c2\perp}$.

Figure 5 shows the phase diagrams $H_{c2\perp}$ versus T obtained from Figs. 4(a) (circles), 4(b) (squares), and 4(c) (full and empty triangles, for H_{c2_u} and H_{c2_l}, respectively).

To quantitatively analyze proximized systems, the formalism presented by Fominov *et al.* in Ref. [21] is typically used. The formalism, based on the quasiclassical Usadel equations which describe the gap- and pair-correlation functions, was originally developed to describe proximity effects in S/N systems, in particular the behavior of T_c as a function of such parameters as layer thicknesses, interface transparency, and diffusion constants. It was extended to S/F hybrids with F a weak ferromagnet in the dirty limit (the mean free path l is the shortest length after the Fermi wavelength), starting from the linearized Usadel equations. In many cases the so-called single-mode approximation (SMA) can be used and the final equations reduce to

$$\ln(t_0) = \Psi\left(\frac{1}{2}\right) - \Psi\left(\frac{1}{2} - \frac{\Omega^2}{2t_0}\right), \tag{1}$$

$$\Omega \tan\left(\Omega \frac{d_S}{\xi_S}\right) = \frac{\gamma}{\gamma_b} \tag{2}$$

where $t_0 = T_c/T_{cS}$ is the critical temperature of the proximized system T_c normalized by the critical temperature of the isolated superconductor T_{cS}, d_S is the thickness of the superconductor, $\xi_S = (2/\pi)\xi_{S0}$ with ξ_{S0} the Ginzburg-Landau coherence length and Ψ the digamma function, and Ω is the pair-breaking parameter responsible for the suppression of T_c. In Eq. (2), Ω depends on γ, which measures the strength of the proximity effect, and on γ_b, which describes the effect of the boundary transparency [22]. These equations allow us to describe the T_c variation as a function of the layer thickness (either of S or F), at zero field. Due to the additivity of the pair breaking [23], it is trivial to extend the formalism to include the role of the magnetic field, as shown in Ref. [24]. In this case in Eqs. (1) and (2) Ω^2 is substituted by

$$\Omega^2(t) = \Omega_0^2 + h_{c2\perp}(t) \tag{3}$$

where $t = T/T_{cS}$ and $h_{c2\perp}(t) = (2\pi/\phi_0)H_{c2\perp}\xi_S^2$. Ω_0^2 is the pair-breaking parameter at zero field. By combining Eqs. (1)–(3) and solving them numerically it is possible to obtain and fit the H_{c2} versus T dependence. Close to T_c (smaller critical fields), the dependence is linear.

The isolated superconductor can be described by the equations above in the limit $\Omega_0 \to 0$. The T_c of MoGe is approximately 6.9 K, close to the bulk value [25]. By fitting the curve we obtain $\xi_S \simeq 2.7$ nm, which gives a coherence length $\xi_{S0} \simeq 4.2$ nm, consistent with what is reported in literature for MoGe [25]. The same result for ξ_{S0} can be obtained from Ginzburg-Landau by the linear relation which describes the perpendicular H_{c2} dependence of a superconducting film near T_c:

$$\mu_0 H_{c2\perp} = \frac{\phi_0}{2\pi\xi_{S0}^2}\left(1 - \frac{T}{T_c}\right) \tag{4}$$

where ϕ_0 is the magnetic quantum flux.

In our trilayer MoGe/Ni/Cu, Ni is a relatively strong ferromagnet (exchange energy $E_{ex} \simeq 200$ meV). This raises the question about the validity of Usadel equations (dirty limit). The two main conditions for the validity are (i) $E_{ex} \ll E_F$, with E_F the Fermi energy, and (ii) $\xi_F = \sqrt{\hbar D_F/E_{ex}} \gg l$, with D_F the diffusion coefficient of F and l the mean free path. If we take a Fermi velocity $v_F = 10^6$ m/s and we calculate D_F from v_F and the experimental resistivity $\rho_{Ni} = 7\,\mu\Omega\,$cm, the estimated values are $E_F \simeq 2.8$ eV, $\xi_F \simeq 1.5$ nm, and $l \simeq 5.4$ nm. While (i) is satisfied, (ii) is not. However, the Ni layer of our system is really thin and the value of l, calculated from the resistivity measured for much thicker films, could be overestimated. If we assume that the Usadel equations are valid and we try to fit the trilayer data with Eqs. (1)–(3), we obtain $\xi_{S0} \simeq 4.5$ nm, a value close to the one of the isolated MoGe, but the T_c suppression from 7.0 to 6.3 K cannot be reproduced. The minimum T_c we can obtain (in the case of very small γ_b) is 6.5 K, a signal that the SMA (often used in the limit of thin superconductors) cannot properly describe our

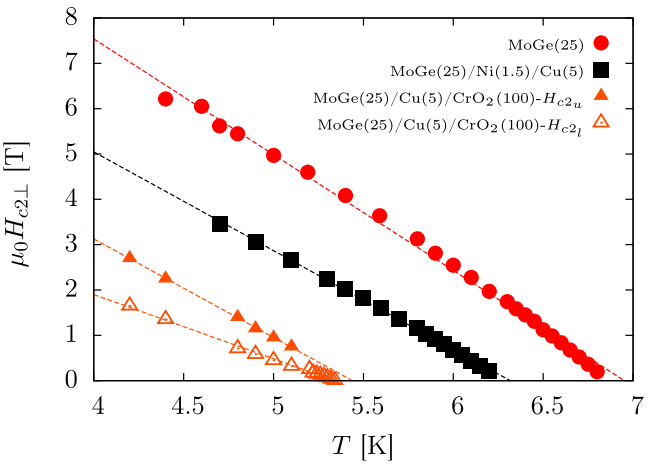

FIG. 5. Phase diagram $H_{c2\perp}$ vs T for the devices of Fig. 4. For MoGe(25) the dashed line results from fitting Eqs. (1) and (2); for the other sets of data it results from fitting Eq. (4).

data. It is possible that the multimode method or the method of fundamental solution [21] could provide more accurate results but more likely a new formalism specifically developed for strong ferromagnets is needed. The analysis above certainly cannot be applied to the trilayer MoGe/Cu/CrO_2 where the proximity is with a thick half-metallic ferromagnet. In this case as expected T_c is suppressed even more, to a value of about 5.4 K.

Even if we cannot have quantitative information about the proximity from the analysis above, we can qualitatively see that the effect of the pair breaking is a simple shift of the $H_{c2}(T)$ curve towards lower T_c values. The slope, dependent only on ξ_S, which is an intrinsic propriety of the superconductor not affected by the pair breaking, should remain unchanged. This is what we observe for the trilayer MoGe/Ni/Cu and for MoGe/Cu/CrO_2, if we consider H_{c2_u}. Instead, $H_{c2_l}(T)$ shows a lower slope. This observation seems to suggest that H_{c2_u} is the proper definition of $H_{c2\perp}$. However, since a certain amount of triplet generation cannot be completely excluded in this case (as mentioned in Sec. III B), the behavior of H_{c2_u} could simply describe the dependence of the superconductor before the CrO_2 gets proximized.

B. $H_{c2\perp}$ of triplet spin valve structures

As we can see from Fig. 6(b) the full TSV shows a behavior very different from the trilayers. In Fig. 6(b) we show the phase diagram for the TSV MoGe(25)/Ni(1.5)/Cu(5)/CrO_2(100) compared with the trilayer MoGe(25)/Cu(5)/CrO_2(100), for

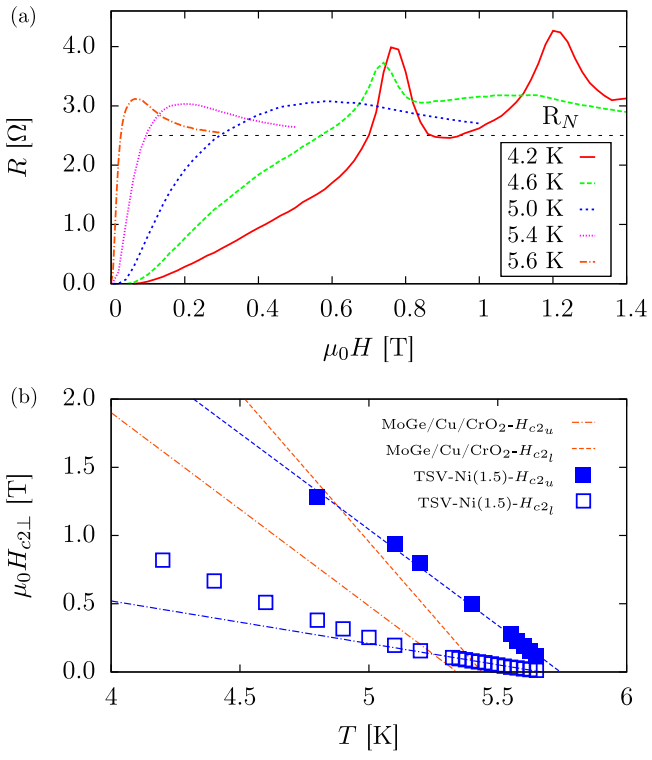

FIG. 6. $R(H)$ curves at different temperatures (a) and phase diagram $H_{c2\perp}(T)$ (b), for the TSV MoGe(25)/Ni(1.5)/Cu(5)/CrO_2(100). (b) Zoom of the curve plotted in Fig. 5(c). The dashed line is the linear fit of the points with $T > 0.85T_c$.

both H_{c2_u} (dashed lines, full squares) and H_{c2_l} (dot-dashed lines, empty squares), defined as described in Sec. IV A [Fig. 4(c)]. A selection of the $R(H)$ transitions for the TSV, from which the values of H_{c2_u} and H_{c2_l} are obtained, is shown in Fig. 6(a). The feature observed, namely, the peak at the onset of the transition and the oscillations visible at around 0.8 and 1.2 T, have been extensively discussed in Secs. III B and IV A.

The critical temperature of the TSV, about 5.7 K, is slightly higher than the trilayer MoGe/Cu/CrO_2 where there is no (or little) triplet generation. This is not consistent with what was expected and with what was observed in Ref. [12] and it is likely due to differences between the interface transparencies of the samples we compare. If we look at H_{c2_u} the relation is linear but with a significantly lower slope, 0.65 times the slope of the trilayer. This suggests that what we observe for a TSV is not simply a pair breaking due to S/F proximity, but a stronger effect due to the leakage of triplets in the ferromagnet. In this case the multilayer behaves more like an S/N than an S/F proximized system.

If we look at H_{c2_l}, the slope is suppressed even more. Here, we see another interesting and unexpected feature: the dependence is linear very close to T_c but at around $T = 0.85T_c$ it strongly deviates to higher values. Interestingly enough, this unusual behavior is pronounced for TSV-Ni(1.5) and TSV-Ni(1.0) and it gradually disappears by increasing or decreasing the Ni thickness. This seems to suggest a relation between nonlinearity and triplet generation. In Sec. IV A we addressed the problem of large oscillations in the transition curves at low temperatures. The lower the temperature (higher critical field) the more oscillation modes are included in the transition. For this reason we have to point out that the values extrapolated at lower temperatures are less precise. However, the range of variation is not such to modify the qualitative behavior of our observation. Moreover at low fields no oscillations are present so that the definition of the slope of the curve is not affected by that. A similar nonlinear behavior has been reported in Ref. [26] for Nb/Cu bilayers. The authors propose several, although not conclusive, explanations for the observation, but in general the effect is attributed to the proximity effect and the boundary conditions. Even if we do not have enough elements to claim that the physical mechanism for the similar behavior is the same, such effects observed in an S/N bilayer seem to be consistent with what we measure in a S/F-type structure with a long-range proximity effect.

If we compare the slope of the phase diagram for TSVs with different Ni thickness, we expect a stronger effect the closer we are to the optimum value. This is confirmed by the experimental results shown in Fig. 7, where we plot the absolute value of the slope obtained by the fit of the $H_{c2_u}(T)$ curves as a function of the Ni thickness. Dashed and dot-dashed lines show the value for the isolated MoGe(25) and the trilayer MoGe(25)/Ni(1.5)/Cu(5), respectively.

As for the T_c variation [Fig. 2(b)], we observe a nonmonotonic behavior, with a maximum effect between 1.0 and 1.5 nm. A similar value has been obtained for the δT_c dependence. This suggests that there is a direct correlation between slope of the $H_{c2_u}(T)$ curve and the TSV efficiency, namely, the triplet generation.

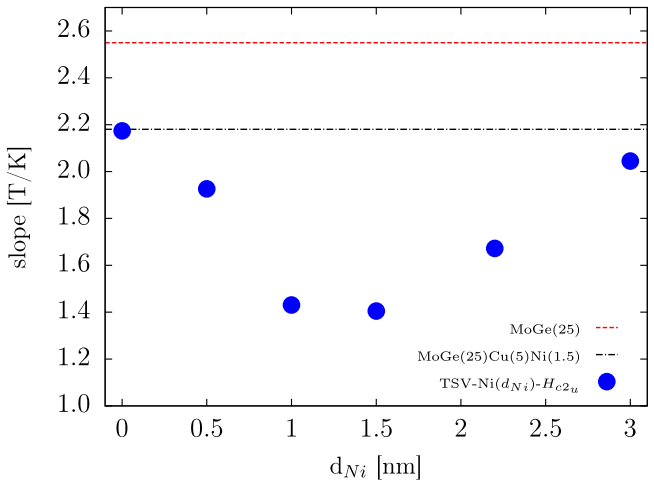

FIG. 7. Slope of the linear fit of curve $H_{c2_u}(T)$ as a function of the thickness of the Ni layer d_{Ni} (squares). Dashed to dot-dashed lines show the value for the isolated MoGe(25) and the trilayer MoGe(25)/Ni(1.5)/Cu(5), respectively.

V. CONCLUSION

To summarize, we showed that for superconducting triplet spin valves based on the half-metallic CrO_2 the efficiency of the singlet to triplet conversion, and thus the magnitude of the spin valve effect, depends on the thickness of the spin mixer layer. In our case the spin mixer is Ni and the optimum value is found to be around 1.5 nm. This dependence has already been shown for other systems such as Josephson junctions based on Co with a similar outcome. However, it has been shown before not in a TSV and it is a further, although indirect, proof of the triplet nature of the observed effects. In addition we addressed the phenomenon of spin accumulation, which we believe can explain the emergence of the peak observed at the onset of the superconductivity for both $R(T)$ and $R(H)$ transitions. Furthermore we studied the dependence of the perpendicular upper critical field as a function of the temperature for a TSV. The determination of the actual H_{c2} value is complicated by the presence of the spin accumulation peak, however we could define an upper and lower limit, H_{c2_u} and H_{c2_l}, which allowed us to compare the TSVs with the systems with no triplet generation. The behavior is very different from the standard S/F proximized systems: the slope is strongly suppressed, similarly to what happens in S/N systems, and for $H_{c2_l}(T)$ we observe a clear deviation from the universal linear dependence. Both effects are prominent for Ni thicknesses around 1.5 nm and vanish for thinner or thicker Ni layers, which indicates a link with the efficiency of the triplet generation. This behavior cannot be described by simple pair breaking, as described by the formalism developed so far for S/F hybrids. A new theoretical formalism along the lines of Ref. [16] is needed to describe the behavior of the critical field in presence of triplet superconductivity.

ACKNOWLEDGMENTS

Technical support from M. B. S. Hesselberth and D. Boltje, and discussions with Y. Fominov, are gratefully acknowledged. This work is part of the research programme of the Foundation for Fundamental Research on Matter (FOM), which is part of the Netherlands Organisation for Scientific Research (NWO). It was supported by a grant from the Leiden-Delft Consortium "NanoFront" and by COST action MP1201.

[1] R. Keizer, S. Goennenwein, T. Klapwijk, G. Miao, G. Xiao, and A. Gupta, Nature (London) **439**, 825 (2006).
[2] M. S. Anwar, F. Czeschka, M. Hesselberth, M. Porcu, and J. Aarts, Phys. Rev. B **82**, 100501(R) (2010).
[3] J. Linder and J. W. A. Robinson, Nat. Phys. **11**, 307 (2015).
[4] F. S. Bergeret, A. F. Volkov, and K. B. Efetov, Phys. Rev. Lett. **86**, 4096 (2001).
[5] M. Eschrig, J. Kopu, J. C. Cuevas, and G. Schön, Phys. Rev. Lett. **90**, 137003 (2003).
[6] M. Houzet and A. I. Buzdin, Phys. Rev. B **76**, 060504(R) (2007).
[7] J. W. A. Robinson, J. D. S. Witt, and M. G. Blamire, Science **329**, 59 (2010).
[8] E. C. Gingrich, P. Quarterman, Y. Wang, R. Loloee, W. P. Pratt, Jr., and N. O. Birge, Phys. Rev. B **86**, 224506 (2012).
[9] T. S. Khaire, M. A. Khasawneh, W. P. Pratt, Jr., and N. O. Birge, Phys. Rev. Lett. **104**, 137002 (2010).
[10] M. Eschrig, A. Cottet, W. Belzig, and J. Linder, New J. Phys. **17**, 083037 (2015).
[11] Y. V. Fominov, A. A. Golubov, T. Y. Karminskaya, M. Y. Kupriyanov, R. G. Deminov, and L. R. Tagirov, JETP Lett. **91**, 308 (2010).
[12] A. Singh, S. Voltan, K. Lahabi, and J. Aarts, Phys. Rev. X **5**, 021019 (2015).
[13] P. V. Leksin, N. N. Garif'yanov, I. A. Garifullin, Y. V. Fominov, J. Schumann, Y. Krupskaya, V. Kataev, O. G. Schmidt, and B. Büchner, Phys. Rev. Lett. **109**, 057005 (2012).
[14] X. L. Wang, A. Di Bernardo, N. Banerjee, A. Wells, F. S. Bergeret, M. G. Blamire, and J. W. A. Robinson, Phys. Rev. B **89**, 140508(R) (2014).
[15] M. G. Flokstra, T. C. Cunningham, J. Kim, N. Satchell, G. Burnell, P. J. Curran, S. J. Bending, C. J. Kinane, J. F. K. Cooper, S. Langridge, A. Isidori, N. Pugach, M. Eschrig, and S. L. Lee, Phys. Rev. B **91**, 060501 (2015).
[16] S. Mironov and A. Buzdin, Phys. Rev. B **92**, 184506 (2015).
[17] M. S. Anwar and J. Aarts, Supercond. Sci. Technol. **24**, 024016 (2011).
[18] J. Wang, M. Singh, M. Tian, N. Kumar, B. Liu, C. Shi, J. K. Jain, N. Samarth, T. E. Mallouk, and M. H. W. Chan, Nat. Phys. **6**, 389 (2010).
[19] M. S. Anwar and J. Aarts, Phys. Rev. B **88**, 085123 (2013).
[20] P. Berghuis and P. H. Kes, Phys. Rev. B **47**, 262 (1993).

[21] Y. V. Fominov, N. M. Chtchelkatchev, and A. A. Golubov, Phys. Rev. B **66**, 014507 (2002).

[22] J. Aarts, J. M. E. Geers, E. Brück, A. A. Golubov, and R. Coehoorn, Phys. Rev. B **56**, 2779 (1997).

[23] Z. Radovic, L. Dobrosavljevicgrujic, A. Buzdin, and J. Clem, Phys. Rev. B **38**, 2388 (1988).

[24] B. Krunavakarn and S. Yoksan, Physica C **440**, 25 (2006).

[25] A. Bezryadin, *Superconductivity in Nanowires: Fabrication and Quantum Transport* (Wiley, New York, 2012), App. A.

[26] A. Sidorenko, C. Surgers, and H. Von Lohneysen, Physica C **370**, 197 (2002).